



Artificial Neural Network Approach for Modeling of Mercury Adsorption from Aqueous Solution by *Sargassum Bevanom* Algae

M. Sharifzadeh Baei^{a*}, R. H. Alizadeh^b

^a Department of Chemical Engineering, Ayatollah Amoli Branch, Islamic Azad University, Amol, Iran.

^b Department of Chemical Engineering, Mazandaran University of Science and Technology, Babol, Iran

PAPER INFO

Paper history:

Received 07 June 2015

Received in revised form 02 July 2015

Accepted 30 July 2015

Keywords:

Mercury

Alga

Adsorption

Thermodynamic

Kinetic

Artificial Neural Network

ABSTRACT

In this study, the adsorption of mercury ions by *Sargassum bevanom* (*S. bevanom*) in batch condition was investigated. SEM was used to study the surface morphology of the biosorbent. The optimum operating parameters such adsorbent dosage, contact time, and pH, were obtained as: a biomass dose of 0.4 g in 100 mL of mercury solution, contact time of 90 min and pH 7. Three equations Morris – Weber, Lagergren and pseudo second order are tested to verify the kinetics of the adsorption process. The data are well explained by the model of Weber Morris. The Langmuir, Freundlich, Temkin, and Dubinin–Radushkevich were subjected to sorption data to estimate sorption capacity; the Langmuir model indicated better performance in the fitting of equilibrium data. Also, the thermodynamic parameters indicated that the adsorption of mercury by *S. bevanom* was spontaneous and endothermic. Artificial Neural Networks (ANN) was used to predict the adsorption efficiency for the removal of mercury ions; the ANN model could estimate the behavior of mercury removal process.

doi: 10.5829/idosi.ije.2015.28.08b.03

1. INTRODUCTION

Heavy metals pollution of natural waters has caused many problems in the past decade. Many factors causing the entry of heavy metals into the environment are considered as serious threat to natural ecosystems such as fossil fuel combustion, industrial waste, chemical manufacturing, mining, painting, etc. [1-3]. Mercury is one of the heavy metals and because of some special features such as evaporation from soil and water and conversion from organic to inorganic forms by bacteria that accumulate in the body of organisms is very important [4].

Mercury is non-biodegradable and toxic, and depending on the level of exposure can include effects such as panic disorder, depression, nausea, vomiting, and shortness of breath in humans [5, 6]. So it is very important to remove heavy metals. Common methods

such as biodegradation [7], nano composites [8], ion exchange [9], reverse osmosis [10], solvent extraction [10], evaporation [10], etc., have been used to remove these ions.

Each of these methods has their advantages and disadvantages and among them adsorption process due to convenience, high efficiency and speed and the availability of the various adsorbents are of most interest.

Many factors such as metal concentration, type of adsorbent, amount of adsorbent, temperature, type of metal etc. are effective in adsorption process that type of adsorbent is of particular importance. Among the various biological adsorbents, algal biomass has attracted much attention due to the cost savings, being less sensitive to environmental factors and impurities etc [11]. To increase the separation efficiency of heavy metals by algae several methods can be used, such as heat treatment, acid treatment and etc. [12].

Artificial neural network (ANN) is a promising alternative modeling method. One of the characteristics

*Corresponding Author's Email: mazyar.sharifzaddeh@gmail.com
(M. Sharifzadeh Baei)

of modeling based on artificial neural networks is that it does not require the mathematical description of the phenomena involved in the process, and might therefore prove useful in simulating and up-scaling complex adsorption systems. The success in obtaining a reliable and robust network depends strongly on the choice of process variables involved as well as the available set of data and the domain used for training purposes [13].

In this study, the separation of mercury by algae has been studied. The effects of amount of biomass, contact time and pH on mercury adsorption were analyzed and adsorption isotherm and kinetics and thermodynamics were studied.

2. MATERIALS AND METHODS

Sargassum bevanom was gathered from the Persian Gulf and after washing with distilled water to remove mud and sand, dried, and stored at room temperature.

Then the acid-treated alga was prepared by transferring the *S. bevanom* into a solution of 0.1 M HCl and stirring the mixture at 200 rpm for 8 hours at room temperature. After centrifugation and washing with physiological saline solution and drying in an oven at 60°C, it was crushed and sieved to pick the particles between 200-300 mesh sizes [13].

Mercury solutions were ready according to standard methods [14]. Solutions of Hg were made ready by dissolving HgCl₂ in distilled water and kept with concentrated H₂SO₄.

2. 1. Instrumentation In this study, scanning electron microscopy ((SEM) (HITACHI) Model S-4160) was used to describe the surface morphology of *S. bevanom* at very high level of magnification. *S. bevanom* was covered with gold and palladium to increase the conductivity. Flame atomic absorption spectrophotometer (Model 929, Unicam) was used to determine the concentration of mercury in aqueous solution.

2. 2. Batch Adsorption Experiments Batch adsorption experiments were performed to study the influence of experimental conditions on the absorption of mercury and determine the conditions for achieving the maximum rate of mercury removal. Isotherms, kinetics and thermodynamic assessments were also done in this section. Adsorption test was carried out in a bottle on a magnetic mixer with agitation speed of 300 rpm and 100 mL of solution was used in each stage. At the end of each stage, adsorbent was filtered through a filter paper and the remaining concentration of mercury in solution was measured. All experiments were performed two times and absorbed concentration was given using the experimental results and the

experimental error was less than 4% and the removal efficiency was determined by Equation (1) :

$$\%Removal = \frac{C_i - C_f}{C_i} * 100 \quad (1)$$

where C_i is the initial concentration ($mg L^{-1}$) and C_f is the final concentration ($mg L^{-1}$). q is the quantity of metal adsorbed per specific amount of adsorbent ($mg g^{-1}$). Adsorption capacity at time t , was determined as follows Equation (2):

$$q_t = \frac{(C_i - C_t)V}{m} \quad (2)$$

where C_i and C_t ($mg L^{-1}$) were the liquid-phase concentrations of solutes at initial and a given time t , V was the Hg solution volume (50 mL) that was stable in each test and m is the mass of *S. bevanom* (g). The amount of adsorption at equilibrium q_e was given by Equation (3):

$$q_e = \frac{(C_i - C_e)V}{m} \quad (3)$$

where C_e ($mg L^{-1}$) was the ion concentration at equilibrium.

2. 3. Artificial Neural Network Modeling

Artificial Neural Networks were developed previously from the basic concept of AI that attempts to simulate the process of human brain and nervous system [15, 16]. They contain a set of mathematical relationships that are used to simulate the process of learning and memory [17]. In recent years, there has been much interest in using neural networks for modeling of chemical and biochemical processes due to their ability to detect the relationships between input and output [18, 19]. Normally, each neural network is composed of input layer, one or more hidden layers and an output layer and each layer of network is composed of neurons. The number of neurons in input and output layers is related to the number of independent and dependent parameters defining the process. The neurons in successive layers are related together through weights.

In this study, the neural network toolbox version 9 of MATLAB, math works Inc. was used to develop the ANN model. In this work, a multilayer feed forward neural network was used. Running of neural networks was performed in two stage, training and testing and the Lavenberg-Marquardt algorithm was used to train the ANN model. The inputs in the model consisted of adsorbent dosage (g), initial mercury concentrations ($mg L^{-1}$), initial solution pH and contact time (min) (Table 1) and the separation efficiency was chosen as the output. All empirical data are divided into three categories: training (70%), validation (15%) and exam (15%). All variables and response were normalized between 0 and 1 to decrease the network error and

higher homogeneous results. The normalization equation applied is as follows:

$$y_n = \frac{y_a - y_{min}}{y_{max} - y_{min}} \quad (4)$$

where y_n , y_a , y_{min} and y_{max} are normalized value, actual value, minimum value, and maximum value, respectively. The ANN model training would be more efficient if preprocessing steps are performed on the input and target data [20].

TABLE 1. Experimental condition for neural network

| pH | Initial concentration | Contact time | dosage |
|----|-----------------------|--------------|--------|
| 1 | 50 | 90 | 0.4 |
| 2 | 50 | 90 | 0.4 |
| 3 | 50 | 90 | 0.4 |
| 4 | 50 | 90 | 0.4 |
| 5 | 50 | 90 | 0.4 |
| 6 | 50 | 90 | 0.4 |
| 7 | 50 | 90 | 0.4 |
| 8 | 50 | 90 | 0.4 |
| 9 | 50 | 90 | 0.4 |
| 10 | 50 | 90 | 0.4 |
| 7 | 50 | 10 | 0.4 |
| 7 | 50 | 20 | 0.4 |
| 7 | 50 | 30 | 0.4 |
| 7 | 50 | 40 | 0.4 |
| 7 | 50 | 50 | 0.4 |
| 7 | 50 | 60 | 0.4 |
| 7 | 50 | 70 | 0.4 |
| 7 | 50 | 80 | 0.4 |
| 7 | 50 | 90 | 0.4 |
| 7 | 50 | 100 | 0.4 |
| 7 | 50 | 90 | 0.05 |
| 7 | 50 | 90 | 0.1 |
| 7 | 50 | 90 | 0.15 |
| 7 | 50 | 90 | 0.2 |
| 7 | 50 | 90 | 0.25 |
| 7 | 50 | 90 | 0.3 |
| 7 | 50 | 90 | 0.35 |
| 7 | 50 | 90 | 0.4 |
| 7 | 50 | 90 | 0.45 |
| 7 | 50 | 90 | 0.4 |
| 7 | 50 | 90 | 0.4 |
| 7 | 70 | 90 | 0.4 |
| 7 | 90 | 90 | 0.4 |
| 7 | 110 | 90 | 0.4 |
| 7 | 130 | 90 | 0.4 |
| 7 | 150 | 90 | 0.4 |
| 7 | 170 | 90 | 0.4 |
| 7 | 190 | 90 | 0.4 |
| 7 | 210 | 90 | 0.4 |

TABLE 2. Results of neural network for prediction of adsorption amount.

| | | Sample | R ² |
|----------|------------|--------|----------------------------|
| 4 neuron | Train | 26 | 9.79426 × 10 ⁻¹ |
| | Validation | 6 | 9.94695 × 10 ⁻¹ |
| | testing | 6 | 9.92443 × 10 ⁻¹ |
| 5 neuron | Train | 26 | 9.19434 × 10 ⁻¹ |
| | Validation | 6 | 9.25806 × 10 ⁻¹ |
| | testing | 6 | 9.56454 × 10 ⁻¹ |
| 6 neuron | Train | 26 | 9.98384 × 10 ⁻¹ |
| | Validation | 6 | 9.92218 × 10 ⁻¹ |
| | testing | 6 | 9.97888 × 10 ⁻¹ |
| 7 neuron | Train | 26 | 9.77853 × 10 ⁻¹ |
| | Validation | 6 | 9.74742 × 10 ⁻¹ |
| | testing | 6 | 9.66541 × 10 ⁻¹ |

In order to assess the integrity of the fit of experimental data and the prediction accuracy of the utilized models, the following equation is used:

$$MSE = \frac{\sum |(q_{exp} - q_{cal}) / q_{exp}| \times 100}{N} \quad (5)$$

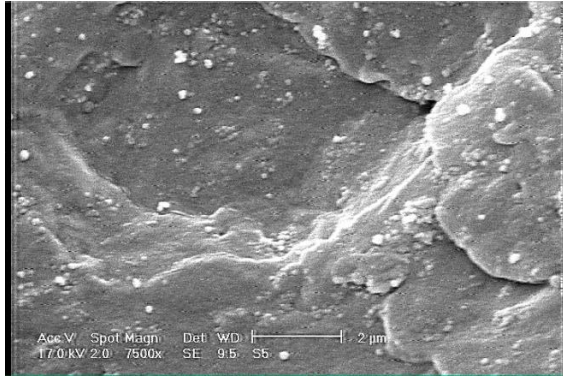
During training, the output vector is computed by a forward pass in which the input variable (pH, initial mercury concentration, contact time and dosage) is propagated forward (Table 1) through the network to compute the output (percentage removal) of each unit. The network is tested with different numbers of neurons to find the optimum number of neurons at hidden layer by observing the R square (R²) (Table 2). The minimum and maximum value of MSE and R² was observed in the number of 6 neurons. Table 2 shows the experimental condition for neural network which pH, initial mercury concentration, contact time and dosage are input variables for network.

3. RESULTS AND DISCUSSION

3. 1. Characterization of the Biosorbent The surface structures of the original and acid-treated *S. bevanom* imaged with different magnifications are shown in Figure 1 (a) - (b). As shown in Figure 1(a) and (b), the original adsorbent was not porous.

3. 2. Effect of pH on Hg (II) Sorption pH is one of the effective parameters on the adsorption process that influences on adsorbent surface charge, degree of ionization, and the species biosorbent [21]. For this reason, the effect of pH on the adsorption of mercury (II) ions on the *S. bevanom* was studied in the range 1-10. Figure 2 shows the effect of pH on the removal efficiency. As can be seen, as pH increases, the absorption of mercury also increases and reaches a

maximum value at pH 7.0, and after that along with increase of pH the removal efficiency reduces. Figure 2 shows a comparison between the ANN model predictions and the experimental data as a function of pH. It can be seen that the ANN model satisfactorily predicts the trend of the experimental data.



(a)



(b)

Figure 1. (a) FE-SEM image of *S. bevanom*. FE-SEM image of *S. bevanom* (b) with more significance

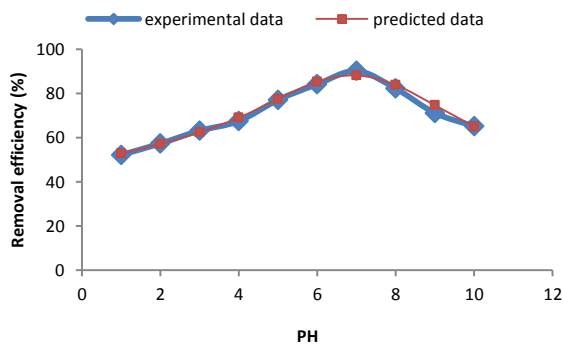


Figure 2. The effect of pH on the removal efficiency and comparison between experimental and predicted data (the initial concentration, contact time, volume of solution and amount of adsorbent were 50 mg L^{-1} , 90 min, 100 mL and 0.4 g, respectively).

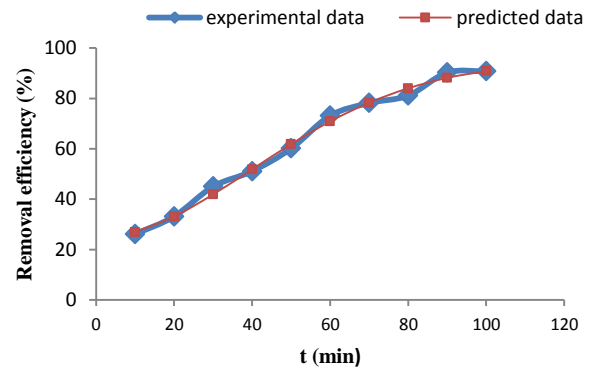


Figure 3. The effect of contact time on the removal efficiency and comparison between experimental and predicted data (the initial concentration, pH, volume of solution and amount of adsorbent were 50 mg L^{-1} , 7, 100 mL and 0.4 g, respectively).

3. 3. Effect of Contact Time

Contact time was obtained as one of the important parameters influencing the adsorption efficiency and the plot of removal efficiency versus the contact time is shown in Figure 3. For these cases, initial Hg (II) concentration was of 50 mg L^{-1} , pH 7 was used for Hg (II). Also, an *S. bevanom* dose of 0.4 g in 100 mL was used. For Hg (II), removal efficiency reached to 90.24% at contact time of 90 min and after that changes were negligible. Thus, the contact time of 90 min was chosen as the optimal time. The agreement between the ANN model predictions and the experimental data as a function of contact time is shown in Figure 3. From this plot, it can be seen that obtained results from the proposed ANN model are in good agreement with the experimental data.

3. 4. Kinetics of Sorption

3. 4. 1. Morris -Weber Kinetic Model

One of the methods to determine whether the absorption process is controlled by the penetration resistance or chemical reaction, using the equation is presented by Morris–Weber. This equation represents a model that the adsorption process is controlled by diffusion [22]. This model is described as follows [23]:

$$q_t = K_{id}(t)^{0.5} + C \tag{6}$$

where q_t is the amount of mercury adsorbed onto the adsorbent at time t (mg/g), K_{id} is the intraparticle diffusion rate constant ($\text{mg g}^{-1} \text{h}^{-0.5}$) and C is the intercept. The plot of q_t vs $(t)^{0.5}$ is given in Figure 4. Constant equation Morris - Weber for mercury $K_{id} = 1292.2 \text{ min}^{-1}$ was calculated from the slope of the straight line and correlation coefficient is 0.9851.

3. 4. 2. Pseudo-second Order Kinetic Model

Pseudo-second order is one of the models in which chemical reactions are controller of absorption. This model is based on equilibrium potential and it is assumed that the filling intensity of adsorbent sites is proportional to the square of the number of vacant adsorbent sites [22]. The equation is represented as Equation (7) [24]:

$$\frac{t}{q_t} = \frac{1}{K_2 q_e^2} + \frac{t}{q_e} \tag{7}$$

where q_t is the amount of mercury ions adsorbed at time t (mg/g) and q_e is the adsorption capacity calculated by the pseudo-second-order kinetic model (mg/g) and K_2 is the second-order adsorption rate constant for the adsorption process ($g/mg.min$). Figure 5 shows the linear plot of pseudo-second-order equation. After linearization, values of k_2 and q_e were calculated using the slope and intercept constant of pseudo-second order equation for adsorption of mercury $K_2 = 7.14 \times 10^{-7} min^{-1}$ and correlation coefficients for mercury is 0.9295.

3. 4. 3. Lagergren Model

Another model that controls adsorption by chemical reaction is Lagergren equation. In this model, filling intensity of adsorbent sites is considered to be linear based on the number of vacant sites and propulsion [22]. Lagergren model is expressed as [25]:

$$\log(q_e - q_t) = \log q_e - \frac{K_1 t}{2.303} \tag{8}$$

where q_e is the adsorption capacity per unit weight of adsorbent at equilibrium and q_t is the amount of mercury ions adsorbed at time t (mg/g), and K_1 is the pseudo first-order rate constant (min^{-1}). The linear plot of $\log(q_e - q_t)$ versus t is shown in Figure 6, and using that the value of K_1 and q_e were calculated. The rate constant $K_1 = 0.0463 min^{-1}$ was calculated with a correlation factor of 0.7404. The results of kinetics are given in Table 3.

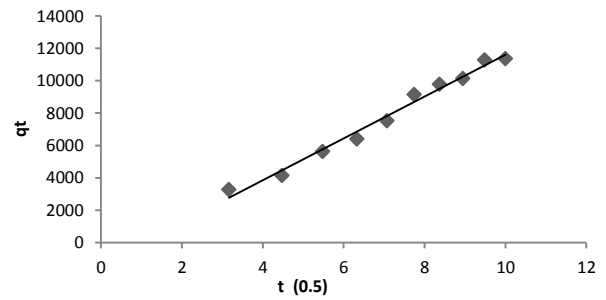


Figure 4. Morris –Weber plot of mercury ions sorption onto *S. bevanom* (the initial concentration, pH, volume of solution and amount of adsorbent were 50 mg L⁻¹, 7, 100 mL and 0.4 g, respectively).

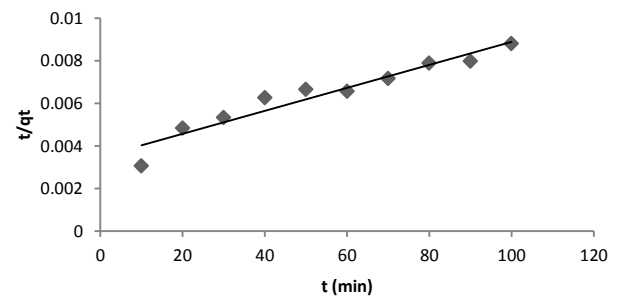


Figure 5. Pseudo-second-order (Type 2) plot of mercury ions sorption onto *S. bevanom* (the initial concentration, pH, volume of solution and amount of adsorbent were 50 mg L⁻¹, 7, 100 mL and 0.4 g, respectively).

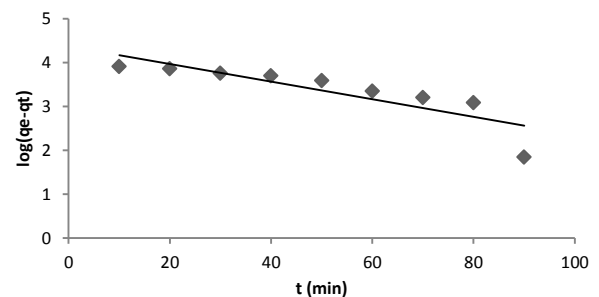


Figure 6. Validation of Lagergren plot of mercury ions sorption onto *S. bevanom* (the initial concentration, pH, volume of solution and amount of ad sorbent were 50 mg L⁻¹, 7, 100 mL and 0.4 g, respectively).

TABLE 3. Kinetic constants for mercury adsorption.

| Pseudo – first order kinetic model | | K (min ⁻¹) | | q _e (mgg ⁻¹) | R ² |
|------------------------------------|--|---|---------------------------|-------------------------------------|----------------|
| | | 0.0463 | | 23302.36 | 0.7403 |
| Pseudo – second order equation | | k ₂ (gmg ⁻¹ min ⁻¹) | | q _e | R ² |
| Type 1 | $\frac{t}{q_t} = \frac{1}{k_2 q_e^2} + \left(\frac{1}{q_e}\right)t$ | t / q _t vs t | 0.000955 | 20000 | 0.9295 |
| Type 2 | $\frac{1}{q_t} = \frac{1}{q_e} + \frac{1}{k_2 q_e^2} \left(\frac{1}{t}\right)$ | 1/ q _t vs 1 t | 2.56 × 10 ⁻⁶ | 12500 | 0.9305 |
| Type 3 | $q_t = q_e - \frac{1}{k_2 q_e} \left(\frac{q_t}{t}\right)$ | q _t vs q _t / t | 1.7 × 10 ⁻⁶ | 14644 | 0.7361 |
| Type 4 | $\frac{q_t}{t} = k_2 q_e^2 - k_2 q_e (q_t)$ | q _t / t vs q _t | 1.0699 × 10 ⁻⁶ | 17103.8 | 0.7361 |
| Morris – Weber equation | | K _{id} (min ⁻¹) | | R ² | |
| | | 0.0007 | | 0.9833 | |

3. 5. Effect of Initial Concentration of Mercury on the Adsorption

To examine the effect of initial concentration on the adsorption of mercury by *S. bevanom*, the experiments were performed at 20°C, with optimum pH and adsorbent dosage and contact time. The initial concentration of mercury solution was 50 mg L⁻¹ which increased to 210 mg L⁻¹ (Figure 7).

The results show that mercury adsorption reduced due to non-availability of active sites required at higher concentrations. Thus, the high absorption at low concentrations was due to these active sites. It can be seen that the ANN model satisfactorily predicts the trend of the experimental data.

3. 6. Effect of Adsorbent Dose

Adsorbent dosage is one of the important and effective parameters for the removal of mercury. Therefore, the effect of adsorbent dose on the absorption was studied at the dose between 0.05 and 0.45 g in 100 mL aqueous solution.

The experiments were carried out at the temperature of 20°C with the optimum pH and the initial mercury ion concentration was 50 mg L⁻¹. As seen in Figure 8 mercury removal rates increased with increasing adsorbent dosage because the surface area increased with increase of the adsorbent. Thus, the optimal dose and mercury removal efficiencies were 0.4 g and 90.09%, respectively. The experimental data and ANN calculated outputs for amount of adsorbent are shown in Figure 8. It can be seen that the ANN model shows a good performance on prediction of the experimental data.

3. 7. The Isotherm Model

Isotherm is based on the assumption that all adsorption sites are identical and independent of the other sites. Also, it shows the relationship between concentrations of adsorbents and the amount of ions adsorbed onto the adsorbent at constant temperature. The collected equilibrium data were fitted with typical isotherm models: Langmuir [25], Freundlich [26], Temkin [27], and Dubinin–Radushkevich [28] isotherm models.

3. 7. 1. The Langmuir Isotherm Model

The Langmuir isotherm model assumes that the adsorption is done in a monolayer and absorption sites located on the

surface of the adsorbent are uniform and all of them have the same absorbing ability. This isotherm model is often offered in the form [25]:

$$q_e = \frac{q_m K_L C_e}{1 + K_L C_e} \tag{9}$$

where q_e is mercury adsorbed per specific amount of adsorbent, C_e is the concentration of the mercury solution (mg L⁻¹) at equilibrium, and q_m is the maximum amount of adsorption of mercury ions (mg.g⁻¹). Langmuir equation can be rearranged to four various linear types as given in Table 4.

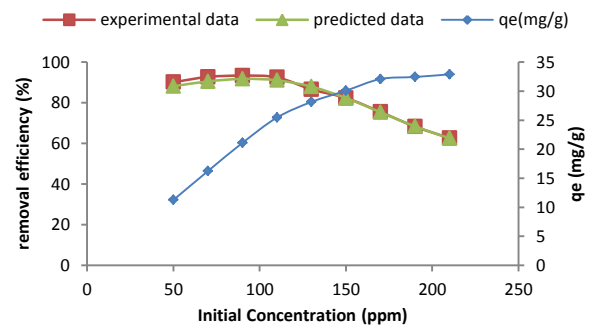


Figure 7. The effect of initial concentration on the adsorption capacity (pH, volume of solution, contact time and amount of adsorbent were 7, 100 mL, 90 min and 0.4, respectively).

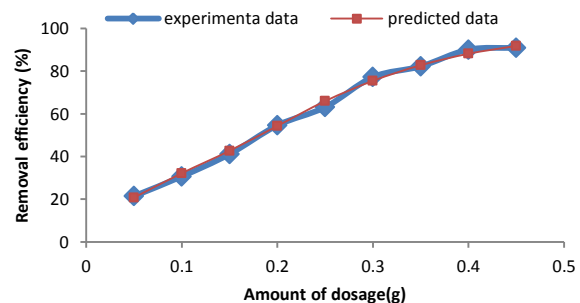


Figure 8. The effect of amount of adsorbent on the removal efficiency and comparison between experimental and predicted data (pH, volume of solution, contact time and initial concentration were 7, 100 mL , 90min and 50 mg L⁻¹, respectively).

TABLE 4. Isotherm constants for mercury adsorption.

| Langmuir equation | K_L (mgL ⁻¹) | q_m (mgg ⁻¹) | R_L | R^2 |
|--|----------------------------|----------------------------|------------------|--------|
| Type 1 $C_e/q_e = K_L/q_m + (1/q_m)C_e C_e/q_e$ vs C_e | 5.6 | 35.59 | 0.003559-0.00085 | 0.9937 |
| Type 2 $1/q_e = K_L/q_m C_e + 1/q_m 1/q_e$ vs $1/C_e$ | 8.68 | 40.82 | 0.0023-0.000548 | 0.7459 |
| Type 3 $q_e = q_m - (K_L) q_e/C_e q_e$ vs q_e/C_e | 4.7812 | 34.343 | 0.087336-0.0001 | 0.5626 |
| Type 4 $q_e/C_e = q_m/K_L - q_e/K_L q_e/C_e$ vs q_e | 8.5 | 41.21 | 0.002348-0.00056 | 0.5626 |
| Freundlich equation | $K n R^2$ | | | |
| Temkin equation $K_T B R^2$ | 3.1046.44810.8222 | | | |
| D - R equation $B q_m R^2 4 \times 10^{-6}$ | 32.6320.9118 | | | |
| | | 10.793.50.7114 | | |

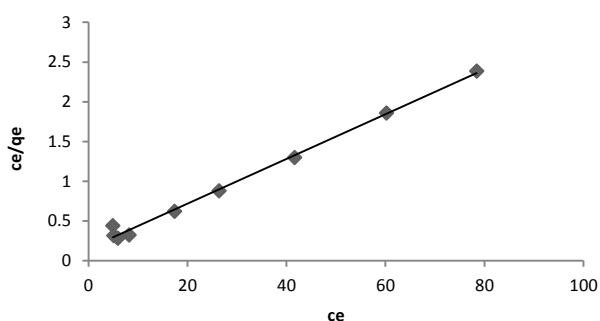


Figure 9. Langmuir sorption isotherm (Type 1) for mercury adsorption onto *S. bevanom* (the initial concentration, pH, volume of solution and contact time was 50 mg L⁻¹, 7, 100 mL and 90 min, respectively)

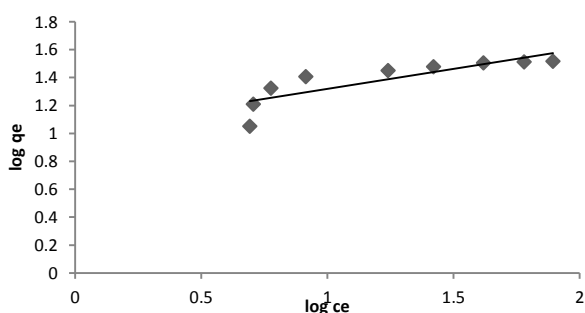


Figure 10. Freundlich sorption isotherm for mercury adsorption onto *S. bevanom* (the initial concentration, pH, volume of solution and contact time was 50 mg L⁻¹, 7, 100 mL and 90 min, respectively).

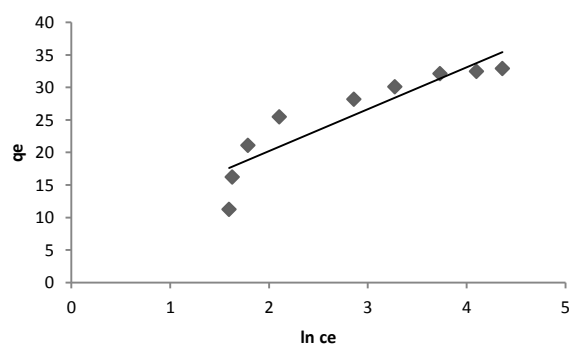


Figure 11. Temkin sorption isotherm for mercury adsorption onto *S. bevanom* (the initial concentration, pH, volume of solution and contact time was 50 mg L⁻¹, 7, 100 mL and 90 min, respectively).

The best fit was obtained by the Langmuir-type 1 compared with other Langmuir models. Figure 9 shows the linear plot Langmuir (Type 1) equation. The basic features and practicality of the Langmuir isotherm regarding a dimensionless constant, separation factor or

equilibrium parameter R_L is defined as Equation (10): [29]:

$$R_L = \frac{1}{1+K_L C_i} \quad (10)$$

where K_L is the Langmuir constant and C_i is the initial concentration of mercury. Desired value of absorption can be between 0 and 1.

3. 7. 2. The Freundlich Isotherm Model The Freundlich isotherm is an empirical model that relates the adsorption intensity of the sorbent relative to the adsorbent [13]. Unlike the Langmuir isotherm, the Freundlich isotherm assumes that the areas on the adsorbent surface are not uniform and have different absorbing ability and absorption energies. This empirical relation is defined as [30]:

$$q_e = K_F (C_e)^{1/n} \quad (11)$$

where K_F is Freundlich isotherm constant associated with adsorption capacity and n is constant proportional to intensity of absorption. The Freundlich equation can be linearized in logarithmic form for the determination of the Freundlich constants as Equation (12):

$$\log(q_e) = \log(K_F) + \frac{1}{n} \log(C_e) \quad (12)$$

Value of K_F was calculated by plotting of $\ln q_e$ versus of $\ln C_e$ (Figure 10). The results are indicated in Table 4.

3. 7. 3. The Temkin Isotherm Model This is an excellent model to predict the equilibrium gas phase, but it is not appropriate. In complex systems such as liquid phase adsorption isotherm [31], this model assumes that the heat absorbed (as a function of temperature) by all of the molecules in the layer, more decreases linearly with respect to the logarithmic [32]. The Temkin isotherm is used usually in the form of Equation (13) [33]:

$$q_e = B L_n (K_T C_e) \quad (13)$$

where $B = \left(\frac{RT}{A_T} \right)$ and K_T is Temkin constant, A_T (J/mol) is the change of the Temkin adsorption energy between two neighboring adsorption sites, T (K) is the adsorption temperature and R (kJ/mol K) is the universal gas constant. The values of K_T and B was calculated with linearization of previous Equation (14) form and plot of q_e versus $\ln (C_e)$ (Figure 11).

$$q_e = B L_n K_T + B L_n C_e \quad (14)$$

The Temkin isotherm model data is shown in Table 4.

3. 7. 4. The Dubinin-Radushkevich Isotherm Model The D-R isotherm model is similar to the

Langmuir isotherm without assuming a homogeneous surface or constant potential of adsorption [28, 34-36]. The linear form of this model is expressed by Equation (15) [28, 34, 35]:

$$L_n q_e = L_n q_m - K \mathcal{E}^2 \quad (15)$$

where q_e is the amount of mercury adsorbed per unit dosage of the adsorbent (mg g^{-1}), q_m is the monolayer capacity, K is the activity coefficient related to mean sorption energy and \mathcal{E} is the Polanyi potential described as Equation (16) [28, 36]:

$$\mathcal{E} = RT L_n (1 + 1/C_e) \quad (16)$$

E (kJ mol^{-1}), the mean energy of sorption is calculated by the following Equation (17) [28, 36]:

$$E = (2K)^{-1/2} \quad (17)$$

By plot of $L_n q_e$ vs \mathcal{E}^2 the values of k and q_m were determined (Figure 12). The results of the isotherm constants are given in Table 4. As our results show, adsorption of mercury by *S. bevanom* can be fitted using Langmuir equations.

3. 8. Adsorption Thermodynamics

3. 8. 1. Effect of Temperature on Adsorption of Mercury

The effect of temperature on the adsorption of mercury on *S. bevanom* was examined at three different temperatures (20, 35, 50 °C).

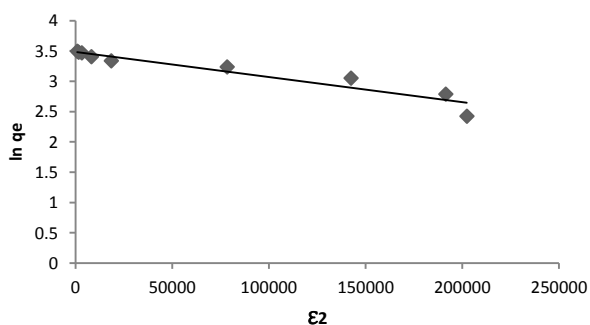


Figure 12. Dubinin–Radushkevick sorption isotherm for mercury adsorption onto *S. bevanom* (the initial concentration, pH, volume of solution and contact time was 50 mg L^{-1} , 7, 100 mL and 90 min, respectively).

TABLE 5. The effect of temperature on the removal efficiency.

| Temperature (°C) | Removal efficiency of mercury (%) |
|------------------|-----------------------------------|
| 20 | 90.12 |
| 35 | 91.45 |
| 50 | 93.65 |

TABLE 6. Thermodynamic parameters for adsorption of mercury onto *S. bevanom*

| ΔH ($\frac{\text{kJ}}{\text{mol}}$) | ΔS ($\frac{\text{kJ}}{\text{mol.k}}$) | T (°C) | ΔG ($\frac{\text{kJ}}{\text{mol}}$) | R^2 |
|---|---|--------|---|--------|
| 12.52 | 0.061 | 20 | -5.3851 | 0.9522 |
| | | 35 | -6.06853 | |
| | | 50 | -7.22676 | |

As given in Table 5, with increasing temperature from 20 to 50 °C the mercury removal efficiencies have risen. This increase indicates that the adsorption process is endothermic. This increase could be attributed to the increased number of active surface sites available on the adsorbent or reducing the thickness of the boundary layer surrounding the adsorbent. The results in Table 5 were used to determine the change in Gibbs free energy (ΔG), the absorption heat (ΔH) and entropy (ΔS) of the adsorption of mercury from aqueous solutions.

3. 8. 2. Effect of Temperature on Thermodynamics Parameter on Adsorption of Mercury

Using the data in Table 4 that show the relationship between temperature and removal efficiency and also the following formula, the parameters of Gibbs free energy (ΔG), enthalpy (ΔH) and entropy (ΔS) were calculated by Equation (18 – 20):

$$K_c = \frac{F_e}{1-F_e} \quad (18)$$

$$\log K_c = \frac{-\Delta H}{2.303RT} + \frac{\Delta S}{2.303R} \quad (19)$$

$$\Delta G = -RT \ln K_c \quad (20)$$

where F_e is the fraction of mercury ions sorbed at equilibrium. Values of (ΔH) and (ΔS) was obtained using the slope and intercept of a linear equation (Equation (19)), and ΔG was calculated by Equation (20). The results are given in Table 6. The positive values of ΔH is indicative of endothermic and negative values of ΔG which shows the spontaneous nature of the adsorption process.

4. CONCLUSIONS

In this study, the efficiency of biomass for the removal of mercury from the aqueous solution in batch mode was investigated and appropriate and optimized data to achieve maximum absorption of mercury obtained in this way are: sorbent dose of 0.4 g in 100 mL of mercury solution, contact time of 90 min and pH 7. Isotherm studies showed that the data are well described

by Langmuir equation. The Morris-Weber's model is the best kinetic model to analyze the data in this study. With investigating the effect of initial concentration of mercury, it was shown that the separation efficiency decreased with increasing the initial concentration. Thermodynamic parameters showed that mercury ions adsorption on to the adsorbent was spontaneous and endothermic. The mercury adsorption yield by *S. bevanom* was predicted by applying a three-layered neural network with 6 neurons in the hidden layer with a good correlation coefficient of 0.99. By comparing the experimental values with the predicted values by ANN in the charts, it was observed that the predicted values were in good agreement with experimental values. The sensitivity analysis showed that MSE values decreased as the number of variables used in the ANN model increased. The present outcome recommend that algae may be used as an economical and effectual adsorbent for the confiscation of Hg(II) ions from aqueous solutions.

5. REFERENCES

- Dong, J., Xu, Z. and Wang, F., "Engineering and characterization of mesoporous silica-coated magnetic particles for mercury removal from industrial effluents", *Applied Surface Science*, Vol. 254, (2008), 3522–3530.
- Meena, A.K., Mishra, G.K., Rai, P.K., Rajagopal, C. and Nagar, P.N., "Removal of heavy metal ions from aqueous solutions using carbon aerogel as an adsorbent", *Journal of Hazardous Materials*, Vol. 122, No. 1–2, (2005), 161-170.
- Jianjun Xie, X.L. and Liang, J., "Absorbency and adsorption of poly(acrylic acid-co-acrylamide) hydrogel", *Journal of Applied Polymer Science* Vol. 106, (2007), 1606-1613.
- Morita, M., Yoshinaga, J. and Edmonds, J.S., "The determination of mercury species in environment and biological samples", *Pure & Applied Chemistry*, Vol. 70, No. 8, (1998), 1585-1615.
- Berglund, F. and Bertin, M., "Chemical fallout", *Springfield: Thomas Publishers*, (1969).
- Krishnamoorthi, C.R. and Vishwanathan, P., Toxic metal in the indian environment, Tata Mc Graw Hill Publishing Co. Ltd., New Delhi. (1991)
- He, Z., Siripornadulsil, S., Sayre, R.T., Traina, S.J. and Weavers, L.K., "Removal of mercury from sediment by ultrasound combined with biomass (transgenic *chlamydomonas reinhardtii*)", *Chemosphere*, Vol. 83, No. 9, (2011), 1249-1254.
- Wan, Q., Duan, L., He, K. and Li, J., "Removal of gaseous elemental mercury over a ceo₂-wo₃/tio₂ nanocomposite in simulated coal-fired flue gas", *Chemical Engineering Journal*, Vol. 170, No. 2–3, (2011), 512-517.
- Verma, V.K., Tewari, S. and Rai, J.P.N., "Ion exchange during heavy metal bio-sorption from aqueous solution by dried biomass of macrophytes", *Bioresource Technology*, Vol. 99, No. 6, (2008), 1932-1938.
- Ahmadpour, A., Tahmasbi, M., Bastami, T.R. and Besharati, J.A., "Rapid removal of cobalt ion from aqueous solutions by almond green hull", *Journal of Hazardous Materials*, Vol. 166, No. 2–3, (2009), 925-930.
- Lodeiro, P., Herrero, R. and Vicente, M.E.S.d., "The use of protonated sargassum muticum as biosorbent for cadmium removal in a fixed-bed column", *Journal of Hazardous Materials*, Vol. 137, No. 1, (2006), 244-253.
- Yang, J. and Volesky, B., "Modeling uranium-proton ion exchange in biosorption", *Environmental Science Technology*, Vol. 33, No. 22, (1999), 4079-4085.
- Esfandian, H., Javadian, H., Parvini, M., Khoshandam, B. and Katal, R., "Batch and column removal of copper by modified brown algae sargassum bevanom from aqueous solution", *Asia-Pacific Journal of Chemical Engineering*, Vol. 8, No. 5, (2013), 665-678.
- "Standard methods for the examination of water and wastewater, ed. 17th, Washington, D.C., American Public Health Association/American Water Works Association/ Water Environment Federation, (1989).
- Chairez, I., García-Peña, I. and Cabrera, A., "Dynamic numerical reconstruction of a fungal biofiltration system using differential neural network", *Journal of Process Control*, Vol. 19, No. 7, (2009), 1103-1110.
- Rene, E.R., Veiga, M.C. and Kennes, C., "Experimental and neural model analysis of styrene removal from polluted air in a biofilter", *Journal of Chemical Technology & Biotechnology*, Vol. 84, No. 7, (2009), 941-948.
- Asl, S.H., Ahmadi, M., Ghiasvand, M., Tardast, A. and Katal, R., "Artificial neural network (ANN) approach for modeling of cr(vi) adsorption from aqueous solution by zeolite prepared from raw fly ash (ZFA)", *Journal of Industrial and Engineering Chemistry*, Vol. 19, No. 3, (2013), 1044-1055.
- Baughman, D.R., Neural networks in bioprocessing and chemical engineering, Y.A. Liu, Editor., Academic Press: San Diego : (1995).
- Sato, A., Sha, Z. and Palosaari, S., "Neural networks for chemical engineering unit operations", *Chemical Engineering & Technology*, Vol. 22, No. 9, (1999), 732-739.
- Aghav, R.M., Kumar, S. and Mukherjee, S.N., "Artificial neural network modeling in competitive adsorption of phenol and resorcinol from water environment using some carbonaceous adsorbents", *Journal of Hazardous Material*, Vol. 188, No. 1-3, (2011), 67-77.
- Park, D., Yun, Y.S. and Park, J.M., "Reduction of hexavalent chromium with the brown seaweed ecklonia biomass", *Environmental Science Technology*, Vol. 38, No. 18, (2004), 4860-4864.
- Katal, R., Hasani, E., Farnam, M., Baei, M.S. and Ghayyem, M.A., "Charcoal ash as an adsorbent for ni(ii) adsorption and its application for wastewater treatment", *Journal of Chemical & Engineering Data*, Vol. 57, No. 2, (2012), 374-383.
- Weber, W.J. and Morris, J.C., "Kinetics of adsorption on carbon from solution", *Journal of the Sanitary Engineering Division*, Vol. 89, No., (1963), 31-59.
- Bhattacharya, A.K., Naiya, T.K., Mandal, S.N. and Das, S.K., "Adsorption, kinetics and equilibrium studies on removal of cr(vi) from aqueous solutions using different low-cost adsorbents", *Chemical Engineering Journal*, Vol. 137, No. 3, (2008), 529-541.
- Langmuir, I., "The adsorption of gases on plane surfaces of glass, mica and platinum", *Journal of the American Chemical Society*, Vol. 40, No. 9, (1918), 1361-1403.
- Freundlich, H., "Of the adsorption of gases. Section ii. Kinetics and energetics of gas adsorption. Introductory paper to section ii", *Transactions of the Faraday Society*, Vol. 28, No. 0, (1932), 195-201.

27. Temkin, M.J. and Pyzhev, V., "Recent modifications to langmuir isotherms", *Acta Physiochim., URSS*, Vol. 12, No., (1940), 217-222.
28. Dubinin, M.M. and Radushkevich, L.V., "Equation of the characteristic curve of activated charcoal", *Chem. Zentr.*, Vol. 1, No., (1947), 875.
29. Azizian, S., "Kinetic models of sorption: A theoretical analysis", *Journal of Colloid and Interface Science*, Vol. 276, No. 1, (2004), 47-52.
30. Esfandian, H., Jafari, M., Alizadeh, M., Rahmati, H.T. and Katal, R., "Synthesis of polyaniline nanocomposite and its application for chromium removal from aqueous solution", *Journal of Vinyl and Additive Technology*, Vol. 18, No. 4, (2012), 250-260.
31. Kim, Y., Kim, C., Choi, I., Rengaraj, S. and Yi, J., "Arsenic removal using mesoporous alumina prepared via a templating method", *Environ Sci Technol*, Vol. 38, No. 3, (2003), 924-931.
32. Aharoni, C. and Ungarish, M., "Kinetics of activated chemisorption. Part 2.-theoretical models", *Journal of the Chemical Society, Faraday Transactions 1: Physical Chemistry in Condensed Phases*, Vol. 73, No. 0, (1977), 456-464.
33. Temkin, M.I., "Adsorption equilibrium and process kinetics on inhomogeneous surfaces with interaction between adsorbed molecules", *Zhurnal Fizicheskoi Khimii*, Vol. 15, No., (1941), 296-332.
34. Katal, R., Vafaie Sefti, M., Jafari, M., Saeedi Dehaghani, A.H., Sharifian, S. and Ghayyem, M.A., "Study effect of different parameters on the sulphate sorption onto nano alumina", *Journal of Industrial and Engineering Chemistry*, Vol. 18, No. 1, (2012), 230-236.
35. Katal, R., Baei, M.S., Rahmati, H.T. and Esfandian, H., "Kinetic, isotherm and thermodynamic study of nitrate adsorption from aqueous solution using modified rice husk", *Journal of Industrial and Engineering Chemistry*, Vol. 18, No. 1, (2012), 295-302.
36. Ramadan, H., Ghanem, A. and El-Rassy, H., "Mercury removal from aqueous solutions using silica, polyacrylamide and hybrid silica-polyacrylamide aerogels", *Chemical Engineering Journal*, Vol. 159, No. 1-3, (2010), 107-115.

Artificial Neural Network Approach for Modeling of Mercury Adsorption from Aqueous Solution by Sargassum Bevanom Algae

RESEARCH NOTE

M. Sharifzadeh Baei^a, R. H. Alizadeh^b

^a Department of Chemical Engineering, Ayatollah Amoli Branch, Islamic Azad University, Amol, Iran.

^b Department of Chemical Engineering, Mazandaran University of Science and Technology, Babol, Iran

PAPER INFO

چکیده

Paper history:

Received 07 June 2015

Received in revised form 02 July 2015

Accepted 30 July 2015

Keywords:

Mercury

Alga

Adsorption

Thermodynamic

Kinetic

Artificial Neural Network

در این تحقیق فرایند جذب یونهای جیوه توسط *Sargassum bevanom* (*S. bevanom*) در فرایند غیر پیوسته مورد بررسی قرار گرفته است. پارامترهای مربوط به شرایط بهینه فرایند از قبیل میزان جاذب، مدت زمان تماس و پ هاش بدین ترتیب تعیین گردید: میزان جرم جاذب بیولوژیکی 0.4 گرم در 100 میلی لیتر محلول جیوه، زمان تماس 90 دقیقه و پ هاش 7. سه معادله موریس-وبر، لاگرگرن و شبه درجه دوم جهت بررسی سینتیک واکنش جذب مورد بررسی قرار گرفتند که روند داده ای آزمایشگاهی تطبیق بالائی با معادله موریس-وبر داشت. همچنین با بررسی مدل های ایزوترم لانگمویر، فرنلیدج، تمکین و دیدینین-رادوچکویچ بر روی داده های جذبی جهت تخمین ظرفیت جذب، معادله لانگمویر پوش مناسبتری بر روی داده های تعادلی داشت. همچنین پارامترهای ترمودینامیکی نشان دادند که فرایند جذب جیوه به وسیله *S. bevanom* گرماگیر می باشد. شبکه عصبی مصنوعی (») جهت تخمین بازده جذب در فرایند حذف یونهای جیوه استفاده گردید.

doi: 10.5829/idosi.ije.2015.28.08b.03